NeuroImage 203 (2019) 116185

Contents lists available at ScienceDirect

NeuroImage

journal homepage: www.elsevier.com/locate/neuroimage

Auditory cortical generators of the Frequency Following Response are modulated by intermodal attention

Thomas Hartmann *, Nathan Weisz

Centre for Cognitive Neuroscience and Department of Psychology, Paris-Lodron Universität Salzburg, Hellbrunnerstraße 34/II, 5020, Salzburg, Austria

ARTICLE INFO

Keywords:
FFR
Brainstem
Auditory cortex
Attention
MEG

ABSTRACT

The efferent auditory system suggests that brainstem auditory regions could also be sensitive to top-down processes. In electrophysiology, the Frequency Following Response (FFR) to speech stimuli has been used extensively to study brainstem areas. Despite seemingly straight-forward in addressing the issue of attentional modulations of brainstem regions by means of the FFR, the existing results are inconsistent. Moreover, the notion that the FFR exclusively represents subcortical generators has been challenged. We aimed to gain a more differentiated perspective on how the generators of the FFR are modulated by either attending to the visual or auditory input while neural activity was recorded using magnetoencephalography (MEG). In a first step our results confirm the strong contribution of also cortical regions to the FFR. Interestingly, of all regions exhibiting a measurable FFR response, only the right primary auditory cortex was significantly affected by intermodal attention. By showing a clear cortical contribution to the attentional FFR effect, our work significantly extends previous reports that focus on surface level recordings only. It underlines the importance of making a greater effort to disentangle the different contributing sources of the FFR and serves as a clear precaution of simplistically interpreting the FFR as brainstem response.

1. Introduction

Analogous to other sensory modalities, neural activity in the auditory system is modulated by selective attention (Frey et al., 2014; Fritz et al., 2007; Mazaheri et al., 2014; Salo et al., 2017; Weise et al., 2016). Electrophysiological research has also focussed on oscillatory activity in cortical brain regions, revealing modulations in the auditory cortex similar to those reported in the visual domain (Händel et al., 2011) or somatosensory regions (Haegens et al., 2011). These findings point to alterations of gain in sensory cortical regions to select or ignore features respectively (e.g. gating by inhibition (Jensen and Mazaheri, 2010)) that are modality-independent (Choi et al., 2013; Frey et al., 2014; Lee et al., 2012). Despite these similarities at the cortical level, compared to the visual modality the auditory system is characterized by a more extensive and complex subcortical architecture, including abundant efferent neural connections (Chandrasekaran and Kraus, 2010; Suga, 2008; Terreros and Delano, 2015; Winer, 2006). Within this efferent system, the primary auditory cortex is a hub region with direct efferent connections to all major subcortical areas (Chandrasekaran and Kraus, 2010; Suga, 2008; Terreros and Delano, 2015; Winer, 2006). In principle, auditory cortical processes could affect cochlear activity via only two synapses (Dragicevic et al., 2015; Suga, 2008; Winer, 2006). These corticofugal modulations are essential in adapting responses of subcortical neurons, for example, by modulating their spectral tuning curves (Felix et al., 2018; Suga, 2008). However, the extent to which subcortical auditory brain regions are implicated in selective attentional modulation is not well established.

Recently, Slee and David (2015) reported attentional modulation of receptive fields of inferior colliculus (IC) neurons in ferrets. In humans functional magnetic resonance imaging (fMRI) has shown modulation of IC activity by selective auditory attention (Riecke et al., 2018; Rinne et al., 2008) and increases of BOLD activity with attentional demand in brainstem structures in an audiovisual attention task (Raizada and Poldrack, 2007). Since all efferent connections to the cochlea are necessarily mediated via the Superior Olive, further suggestive support for subcortical attentional modulations can be derived from studies on otoacoustics emissions (OAEs), a proxy for outer hair cell activity in the cochlea. Attentional modulations of OAEs have been found when either the left or the right ear had to be attended (Giard et al., 1994), one out of two frequencies was task relevant (Maison et al., 2001) or attention had to be focused on the visual or auditory modality (Wittekindt et al., 2014). While limited in number, these studies in animals and humans suggest the sensitivity of brainstem structures to selective attention. However,

* Corresponding author.
E-mail addresses: thomas.hartmann@th-ht.de (T. Hartmann), nathan.weisz@sbg.ac.at (N. Weisz).

https://doi.org/10.1016/j.neuroimage.2019.116185
Received 17 June 2019; Received in revised form 3 September 2019; Accepted 10 September 2019
Available online 11 September 2019
1053-8119/© 2019 The Authors. Published by Elsevier Inc. This is an open access article under the CC BY license (http://creativecommons.org/licenses/by/4.0/).

the picture remains incomplete. Studies in the animal model are only suggestive that similar processes also exist in humans. At the same time invasive recordings from brainstem structures are not feasible in healthy humans. Studies using fMRI studies are non-invasive and provide excellent spatial resolution. Yet, scanner noise creates a challenging environment for such studies, and the technique is also not well suited for some populations in which the study of brainstem processes may be of interest (e.g. cochlear implant patients). Furthermore, the aforementioned complex auditory corticofugal architecture strongly suggests complex interactions of the areas and nuclei involved which can only be captured with recording methods providing high temporal resolution. Therefore other methods are needed to complement the invasive and neuroimaging approaches.

A popular method to noninvasively assess auditory neural activity with high temporal resolution is to use magnetoencephalography (MEG) and/or electroencephalography (EEG). Convincingly capturing attentional modulations of subcortical auditory regions using these techniques has proven challenging, however. Many initial studies focussed on the components of the auditory brainstem response (ABR) (Jewett et al., 1970). The ABR is the evoked response to a high number of repetitions (typically 2000–6000 (Skoe and Kraus, 2010)) of a short sound like a click. The ABR peaks have been related to the processing of the sound at the various subcortical nuclei (Boston and Møller, 1985; Chandrasekaran and Kraus, 2010; Don and Eggermont, 1978; Jewett et al., 1970; Møller et al., 1981; Møller and Burgess, 1986; Møller and Jannetta, 1983; Skoe and Kraus, 2010). It has been used to study plasticity processes of the subcortical auditory system (Chandrasekaran et al., 2014; Chandrasekaran and Kraus, 2010; Kraus and Nicol, 2014; Musacchia et al., 2007; Tzounopoulos and Kraus, 2009) and is widely applied in clinical settings (Eggermont et al., 1980; Eggermont and Don, 1986; Eggermont and Salamy, 1988; Møller and Møller, 1983; Stipdonk et al., 2016; van Straaten, 1999). However, attentional modulation of ABR components have not been found thus far (Hackley et al., 1990; Woldorff et al., 1987).

Another way to use EEG to eavesdrop on subcortical activity is to investigate neural responses to complex sounds such as simple consonant-vowel combinations (e.g. /da/ sound). While the transient part is equivalent to the classical ABR, the sustained part is an oscillatory response that is strictly phase-locked to the stimulus, in particular its fundamental frequency (F0) (Akhoun et al., 2008; Chandrasekaran and Kraus, 2010; Galbraith et al., 1995; Greenberg, 1980; Russo et al., 2004; Skoe and Kraus, 2010). This sustained response, commonly named the frequency-following response (FFR), is assumed to be mainly generated by subcortical auditory nuclei, with the IC playing a central role (Batra et al., 1986; Chandrasekaran and Kraus, 2010; Worden and Marsh, 1968). Support for this notion has come from studies in animals (Liu et al., 2006; Marsh et al., 1974; Rouiller et al., 1979; Wallace et al., 2007). Given these findings and the general notion that the auditory cortex does not track or hardly tracks frequencies beyond 100 Hz (Chandrasekaran and Kraus, 2010; Kuwada et al., 2002), the FFR has thus been seen as a proxy to subcortical auditory activity. Past studies on the attentional modulation of the FFR have found inconsistent results. While evidence of said attentional modulation exists (Forte et al., 2017; Galbraith et al., 2003; Lehmann and Schönwiesner, 2014), negative results have been reported as well (Hoormann et al., 2004; Varghese et al., 2015). It should be noted that all mentioned studies used data from a small number of EEG electrodes, sometimes only one. Since the subcortical generation of the FFR has been widely accepted, the presence or absence of attentional modulations in the aforementioned studies has been attributed to subcortical structures without much scrutiny.

However, besides the general controversy pertaining to its attentional modulation, the view of an exclusive brainstem localization of the FFR has been recently challenged by Coffey and colleagues (Coffey et al., 2016b) for human participants (for similar guinea pig data see (Wallace et al., 2000)). Using MEG and EEG concurrently, they confirmed that the ABR can be acquired with MEG as previously shown by Parkkonen and colleagues (Parkkonen et al., 2009). More importantly, they showed that the FFR can be acquired with MEG as well, as long as the device uses magnetometers. Using source projection, FFR activity was present in all auditory subcortical nuclei (i.e. brainstem and thalamic) but most importantly significant auditory cortical contributions were also identified. The latter finding has important implications concerning past studies using the FFR. If the FFR has cortical components, it is certainly possible that any reported attentional effect could have cortical origins instead of or in addition to subcortical ones. It clearly follows that assertions concerning the source of any effect in an FFR paradigm should be backed up by source analysis techniques (Gross et al., 2001; Hämäläinen and Ilmoniemi, 1994; Lin et al., 2006; Van Veen et al., 1997). Additionally, reporting the temporal dynamics of the FFR along with the reported effects becomes crucial, which is not common in current practice (e.g. (Galbraith et al., 2003; Lehmann and Schönwiesner, 2014; Varghese et al., 2015)). The usual approach of calculating and analysing one spectrum for the whole duration of the sustained part of the original stimulus assumes that contributions from different parts of the auditory hierarchy remain the same which is clearly not the case (Tichko and Skoe, 2017). In order to scrutinize the subcortical and cortical effects of attention on the FFR, we acquired data with whole-head MEG in a cross-modal attention paradigm. We confirmed the strong cortical contributions to the FFR as reported by Coffey and colleagues (Coffey et al., 2016b) and furthermore showed that attentional modulations of the FFR affects only cortical regions.

2. Materials and methods

2.1. Participants

38 volunteers (19 females) took part in the experiment and provided written informed consent. At the time of data acquisition, the average age of the participants was 24.4 years (SD: 6.1). Two of these participants had to be excluded because not all six runs were recorded. One participant was excluded because of excessive power in the time frequency data. One further participant was excluded because more than six sensors were marked as bad by the RANSAC algorithm. The final sample of participants included 34 volunteers (19 females) with an average age of 24.4 years (SD: 6.3). All participants reported no previous neurological or psychiatric disorder, and reported normal or corrected to normal vision. The experimental protocol was approved by the ethics committee of the University of Salzburg and was carried out in accordance with the Declaration of Helsinki.

2.2. Stimulation paradigm

Stimulation was controlled by a custom Matlab script using the Psychophysics Toolbox (Brainard, 1997; Kleiner et al., 2007). Auditory stimuli and triggers were generated and emitted via the VPixx System (DATAPixx2 display driver, PROPixx DLP LED Projector, TOUCHPixx response box by VPixx Technologies, Canada), which was also used to collect the participants' responses. Previous tests of the setup using the Blackbox2 Toolkit (The Black Box ToolKit Ltd, Sheffield, UK) showed that this setup is virtually free of any timing inaccuracies, with jitters of less than 1 ms.

The participants performed six runs of a crossmodal attention task (see Fig. 1). For each of the 85 trials, an attentional cue indicated whether the participant had to react to a rare oddball in either the visual or auditory domain. Each trial started with a central fixation cross, presented for 500 ms followed by the attentional cue (picture of an eye or an ear) presented for 500 ms. A fixation cross appeared for 1000 ms, followed by the audiovisual stimulation. The auditory stimulation consisted of 30 repetitions of a /da/ sound with an effective fundamental frequency of 114 Hz, lasting 40 ms (King et al., 2002; Skoe and Kraus, 2010). As suggested by Skoe and Kraus (2010), the polarity of half the stimuli was reversed to minimize possible stimulus artifacts and cochlea microphonics. Each presentation of the/da/sound was followed by 50 ms of silence. For the duration of the auditory stimulation, a vertically oriented

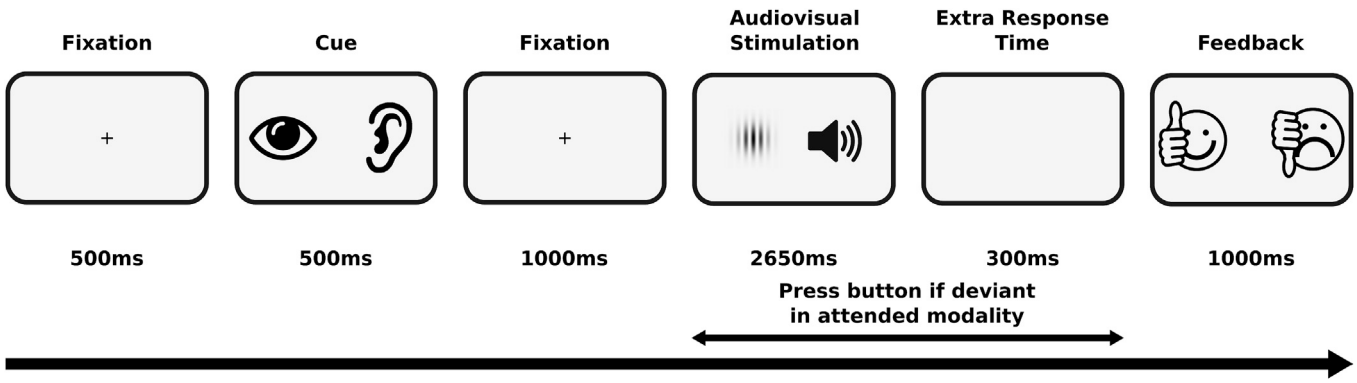

Fig. 1. Timeline of the trials of the experimental paradigm.

gabor patch (visual angle: spatial frequency: 0.01 cycles/pixel, sigma: 60) was presented at the center of the screen. Of the 85 trials, 8 were randomly chosen to be visual oddball trials. Another 8 trials were independently chosen to be auditory oddball trials. Because the oddball trials were chosen independently, some trials were both visual and auditory oddball trials. In visual oddball trials, the gabor patch was tilted by 10° to the left for 270 ms anywhere during the presentation time. In auditory trials, three consecutive presentations of the/da/sound were reversed. The participants had to press a button with their right thumb if the current trial was an oddball trial of the cued modality. They were allowed to answer as soon as the oddball occurred. After the audiovisual stimulation had finished, participants were given an additional 300 ms to answer in order to account for oddball trials in which the oddballs appeared towards the end. After each trial, a smiley was presented for 1000 ms, indicating whether the (non)response of the participant was correct or incorrect.

The total duration of the stimulation was 49 min excluding breaks and preparation. The total amount of stimuli was 15,300.

2.3. Data acquisition

Before entering the shielded room, five head position indicators (HPI) coils were applied on the scalp. Anatomical landmarks (nasion and left/right pre-auricular points), the HPI locations, the position of the 128 EEG channels and around 300 headshape points were sampled using a Polhemus FASTTRAK digitizer.

Concurrent acquisition of the magnetic and electrical signal was performed at a sampling frequency of 5000 Hz (hardware filters: 0.1–1600 Hz) using a whole-head MEG system (Elekta Neuromag Triux, Elekta Oy, Finland), placed in a magnetically shielded room (AK3b, Vacuumschmelze Hanau, Germany). Brain activity was sampled from 102 magnetometers, 204 orthogonally placed gradiometers. 128 EEG channels were additionally acquired from a subset of 31 participants. The remaining 7 participants were equipped with a single EEG electrode at Cz. The ground was placed on the participants' neck and the reference electrode on the left earlobe. Only the data from the magnetometers are reported due to their greater sensitivity to deep sources as compared to gradiometers. The data quality of the EEG recording was not sufficient for the analysis. Many EEG channels showed intermittent periods of high noise for reasons unknown to us. One possibility is that the EEG cap was likely to touch the MEG helmet. This might have compressed the electrode gel. Furthermore, small movements that would not normally lead to noticeable artifacts in the data might have been augmented because pressure on the gel (and thus the impedance between the sensors and the scalp) would be affected.

2.4. Data preprocessing

Preprocessing of the MEG data was done in a two-step approach. In a first step Signal Space Projection (SSP) was applied to remove exogenous contaminations (Uusitalo and Ilmoniemi, 1997). Further data cleaning was performed using a fully automated approach implemented in the autoreject package (version 0.1 running on Python 3.6.8) (Jas et al., 2017, 2016). Specifically, we used autoreject to identify bad sensors and periods containing artifacts, which were subsequently discarded. Because common artifacts in MEG data are found in rather low frequencies, the data of each run were bandpass filtered between 1 and 40 Hz (FIR filter with hann window, low transition width: 0.1 Hz, high transition width: 4 Hz, filter length: 165001). The filtered data were then split into epochs of 1s because the algorithms provided by autoreject require epoched data. Each epoch was further downsampled to 500 Hz to increase the speed and decrease the computational demands of the artifact identification algorithms. We first applied the RANSAC algorithm to identify sensors that contained data that were highly dissimilar to those of the other sensors (Bigdely-Shamlo et al., 2015; Fischler and Bolles, 1981; Jas et al., 2017). If a sensor was marked as bad by the RANSAC algorithm in one run, the sensor was excluded for all runs of the respective participant. If the total number of bad sensors exceeded five, the data of the participant were rejected, leading to the exclusion of one participant. The remaining data were subjected to the "local autoreject" algorithm (Jas et al., 2017, 2016) to identify which of the 1s periods contained artifacts. The exact parameters for the RANSAC and "local autoreject" algorithms can be found in the supplementary material. Each 1s period that was marked as bad by the algorithm was discarded from further analysis. Subsequent analysis on cleaned data was carried out using the open source MNE-Python toolbox (version 0.17.2 running on Python 3.6.8) (Gramfort et al., 2014, 2013). Statistical analysis was performed using Eelbrain version 0.29.5 (Brodbeck, n.d.). Perceptually uniform colormaps ((Kovesi, 2015); (Bedna, n.d.)) were used for all color-coded figures.

We bandpass filtered (FIR filter with hann window, passband: 80–2000 Hz, low transition width: 5 Hz, high transition width: 100 Hz, filter length: 3301) the raw data, followed by a bandstop filter to eliminate line noise contamination (FIR filter with hann window, stop bands at 50 Hz and multiples up to 1950 Hz, transition width: 1 Hz, filter length: 33001). We extracted epochs of data in the time window of 60 ms before to 130 ms after the onset of each individual auditory stimulus, accounting for a 16 ms delay introduced by the tubes of the MEG-proof sound system and 7 ms delay inherent to the sound file we used. In order to reduce possible contamination of the auditory signal by the visual evoked response, the first four auditory stimuli of every trial were discarded, decreasing the number of trials per participant by 2040. We further discarded all trials that occurred within a sequence containing an oddball stimulus. The number of oddball trials was not constant because the 8 oddball sequences per modality were allowed to overlap. On average, this lead to the exclusion of 2387 (SD: 54) trials. False responses were rare (see Behavioral Results) but lead to the exclusion of further 16 (SD: 38.3) trials on average. An average of 601 trials (SD: 650,3) had to

be further removed because the autoreject algorithm had identified an artifact in that time-window. The average amount of trials remaining after this process was 10256 (SD: 650).

The amount of remaining trials within the two conditions did not differ significantly according to a dependent samples *t*-test (visual attention: 5125,3 (SD: 348,1); auditory attention: 5130,8 (SD: 361,8); $T = -0.114$, $p = 0.91$, $df = 33$). However, we noted that significantly more trials belonging to the visual condition were removed because they were presented within an oddball sequence (dependent samples *t*-test: $T = 2.3$, $p = 0.03$, $df = 33$), while the opposite was true for the artifact based exclusion (dependent samples *t*-test: $T = -3.41$, $p = 0.002$, $df = 33$). In order to ensure that our results were not affected by any inequalities, the number of trials within each condition and polarity was equalized. Trials were chosen so that the remaining trials would be as close as possible in time. The final average amount of trials used for the analysis was 10020 (SD: 704.7).

The remaining trials were averaged within their respective condition (attend visual/attend auditory) over both polarities. A further average of all trials of each participant was calculated in order to locate the FFR in time, frequency and space.

2.5. Sensor space analysis

We applied a wavelet transform around the fundamental frequency of the stimulus (Morlet Wavelets, six cycles, 104–124 Hz, $\Delta f = 2$ Hz, $\Delta t = 1$ ms) on the averaged data. In order to exclude any remaining outliers from the analysis, the resulting power values were averaged within each participant. The individual power values were Z-transformed and those participants whose average power was three standard deviations below or above the group average were excluded. This lead to the exclusion of one participant ($z = 4.89$). We computed the power envelope of the FFR by first averaging over all frequency bins.

In order to visualize the FFR on sensor level, the power values were first averaged over all remaining magnetometers within every participant. The average power and standard deviation over all participants was subsequently calculated and resulted in an FFR response peaking at 50 ms after stimulus onset as shown in Fig. 2a.

In order to test our principle hypothesis that FFR activity was higher when the auditory modality was attended, we applied a cluster-based nonparametric, threshold free permutation-based statistic (Maris and Oostenveld, 2007; Smith and Nichols, 2009) (dependent samples *t*-test, 10000 permutations, channel neighborhood structure provided by MNE Python) to the data, restricted to the time-window between stimulus onset to 90 ms later.

2.6. Source space analysis

Nine of the 35 participants included in the final analysis provided us with high-quality T1 MR images. These MRIs were segmented with Freesurfer (Fischl, 2012). Alternatively, the average brain provided by Freesurfer (fsaverage) was morphed to the participants' headshape. The surface of the inner skull was either extracted using Freesurfer (Fischl, 2012) if the individual anatomical images were available or determined by applying the transforms used for morphing the average brain to the participants' headshapes. The coordinate frames of the MR images and the MEG sensor positions were coregistered using MNE Python (Gramfort et al., 2014, 2013). We subsequently computed a one-layer boundary-element model (BEM) (Akalin-Acar and Gençer, 2004) to accurately model the propagation of magnetic fields from generators in the brain to the sensors. We constructed the cortical source space using 4098 sources, each covering approximately 24 mm^2. In order to estimate activity at the brainstem and the thalamus, the surface-based source space was combined with a volumetric source space, placing equidistant source of 5 mm spacing in the regions labeled "Brainstem", "Left-Thalamus-Proper" and "Right-Thalamus-Proper", as defined in the "aseg" atlas (Filipek et al., 1994; Fischl, 2012; Seidman et al., 1999). Further cortical regions of interest (ROI) were defined using the HCP-MMP1.0 atlas (Glasser et al., 2016) morphed to the individuals' anatomy. Similar to Coffey and colleagues (Coffey et al., 2016b), we used the Primary auditory cortex (A1) as the cortical ROI and defined the orbitofrontal cortex (OFC) as the control region. Evoked sensor space activity was projected to the defined sources using the Minimum Norm Estimate method (MNE) (Hämäläinen and Ilmoniemi, 1994). The MNE is known to be biased towards superficial sources. One commonly used way to counteract this bias is to enhance the deeper sources using a depth weighting (Lin et al., 2006). Coefficients between 0.6 and 0.8 have been reported to produce optimal results. In this study, we used a depth weighting coefficient of 0.8. We subsequently applied a wavelet transform with the same parameters used in the sensor space analysis to all orientations of every source the data were projected to. The power values within each source were combined by summing the values of the three orientations. As for the sensor space data, we obtained the power envelope of the FFR by averaging the power over all frequency bins. This approach resulted in data for sources on the cortical surface and the previously defined subcortical regions. In order to assess cortical contributions to the FFR and the attention effect, we morphed these cortical sources to the average brain (fsaverage) provided by Freesurfer. To visualize the cortical attention effect, we calculated T-values (dependent samples, one tailed). For the subsequent ROI analysis, we averaged the power time-courses of each source belonging to each of the ROIs defined above.

The first question we wanted to answer was whether FFR-related activity was higher in the cortical and subcortical auditory regions compared with the two control regions (OFC, left and right hemisphere). We therefore averaged the power of the two control regions. We then applied the same cluster-based, threshold-free permutation statistics (Maris and Oostenveld, 2007; Smith and Nichols, 2009) (dependent samples *t*-test, 10000 permutations, one-tailed) that we used for the sensor data to contrast the power of each of the putatively auditory ROIs with the power of the averaged control region.

The second and crucial question we tried to answer was which of the ROIs were affected by the attentional modulation. We therefore contrasted the power during auditory vs. visual attention at each of the ROIs individually, again using the same cluster-based, threshold-free permutation statistics (Maris and Oostenveld, 2007; Smith and Nichols, 2009).

3. Results

3.1. Behavioral Results

Behavioral response data showed that participants gave the correct response in 99% (SD: 0.7%) of the trials. When an oddball was presented in the cued sensory domain, participants correctly gave a response in 95% (SD: 3.1%) of the respective trials. False responses to oddballs without triggers were given in only 0.1% (SD: 0.3%) of the trials.

3.2. Sensor space analysis

In a first step, we analyzed the temporal dynamic of the FFR in sensor space and subsequently compared the data acquired during the "attend auditory" and the "attend visual" condition. The power envelope showed an evoked response to the sound stimulus peaking at ~50 ms after stimulus onset (see Fig. 2B). The topography of the response shows a bilateral activation pattern, mostly over temporal regions, lateralized to the right hemisphere (see Fig. 2A). Since meaningful control regions cannot be defined on the sensor level, we refrained from further statistical analysis.

The cluster-based nonparametric, threshold-free permutation-based statistics for the impact of the attentional modulation shows that the FFR response is significantly larger when attention is focused on the auditory domain ($p = 0.017$, see Fig. 3B). The effect is, however, restricted to a rather short and late period after stimulus onset (65 ms–80 ms). It also does not coincide with the maximum of the FFR itself. This low power

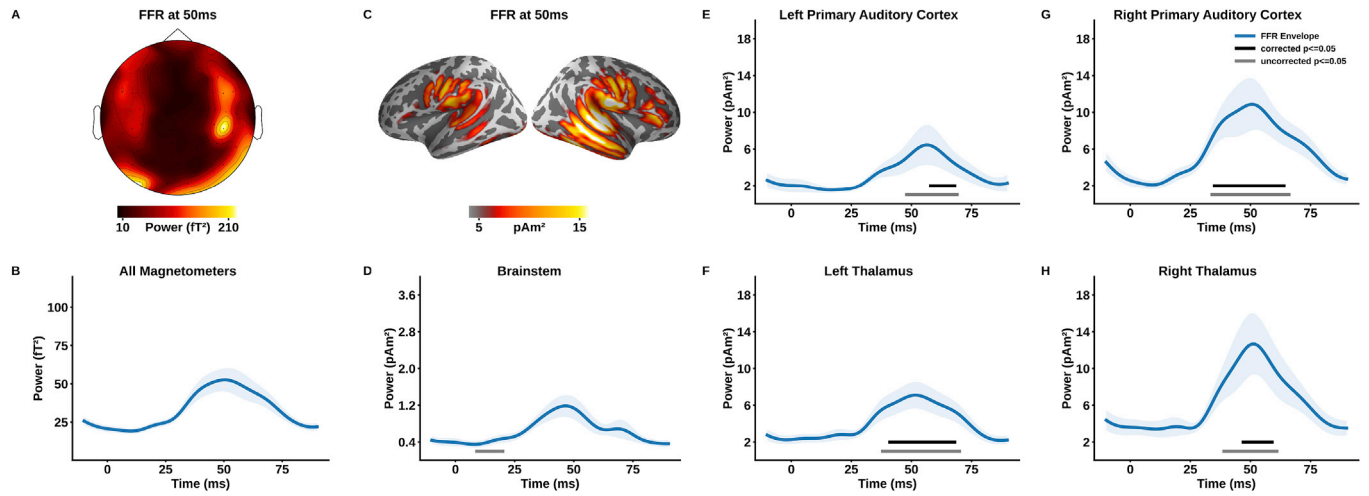

Fig. 2. The Frequency Following Response (FFR) in sensor and source space. A) Topography of the FFR at the time of maximum power. B) Timecourse of the evoked response at the fundamental frequency (f0) of the stimulus averaged over all magnetometers. Shaded error bars denote the standard error. C) Source reconstruction of the FFR at the time of maximum power. D-H) Timecourse of the evoked response at the f0 for the 5 ROIs. Shaded error bars represent the standard error. The black bar at the bottom of each panel represents the temporal extents of the clusters in which the respective ROI showed a higher response than the orbitofrontal cortex, used as a control region. The gray bar at the bottom represents the samples for which the uncorrected p-value of the *t*-test was below 0.05.

and specificity is likely due to an interaction between the low spatial specificity of the magnetometers and the fact that the average over all magnetometers was analyzed. Fig. 3A shows the topography of the comparison between the two conditions at the time of the maximum power of the FFR. It suggests a weak overlap with the topography of the FFR itself (see Fig. 2A). This analysis confirms the presence of the FFR in sensor space and is suggestive yet not conclusive with respect to its modulation by selective (intermodal) attention.

3.3. Source space analysis

After confirming the presence of the FFR as well as finding suggestive evidence for the hypothesized attentional modulation in sensor space, the next step was to locate the respective generators. Importantly, we wanted to reveal possibly different contributions by cortical and subcortical sources. Source projection of the FFR showed strong cortical contributions, lateralized to the right hemisphere (See Fig. 2C). The maximum power was found at the Auditory 4 complex, an auditory region ventral to the primary auditory cortex. The activity is rather widespread, including the primary auditory cortex as well as ventral temporal, parietal and prefrontal regions. The ROI analysis statistically confirmed this notion (see Fig. 2D–H). All five ROIs showed responses to the stimulus at its fundamental frequency. In order to quantify whether the response was specific to the ROI, the envelope at each ROI was statistically contrasted to the envelope at a control region in the orbitofrontal cortex. This analysis showed that all ROIs except the Brainstem generated a significantly stronger FFR than the control region (see Fig. 2). The time periods of the significant increases of these ROIs were well within the range of the sensor-level FFR (for details see Supplementary Table 1).

The cortical areas showing attentional modulation of the FFR are mostly restricted to the right hemisphere and cover early auditory regions as well as regions in the temporo-parieto-occipital junction, the lateral prefrontal cortex and ventral parietal areas (see Fig. 3C). These regions also strongly overlap with those found to show general FFR-related activity. The ROI analysis indicated that the attention effect

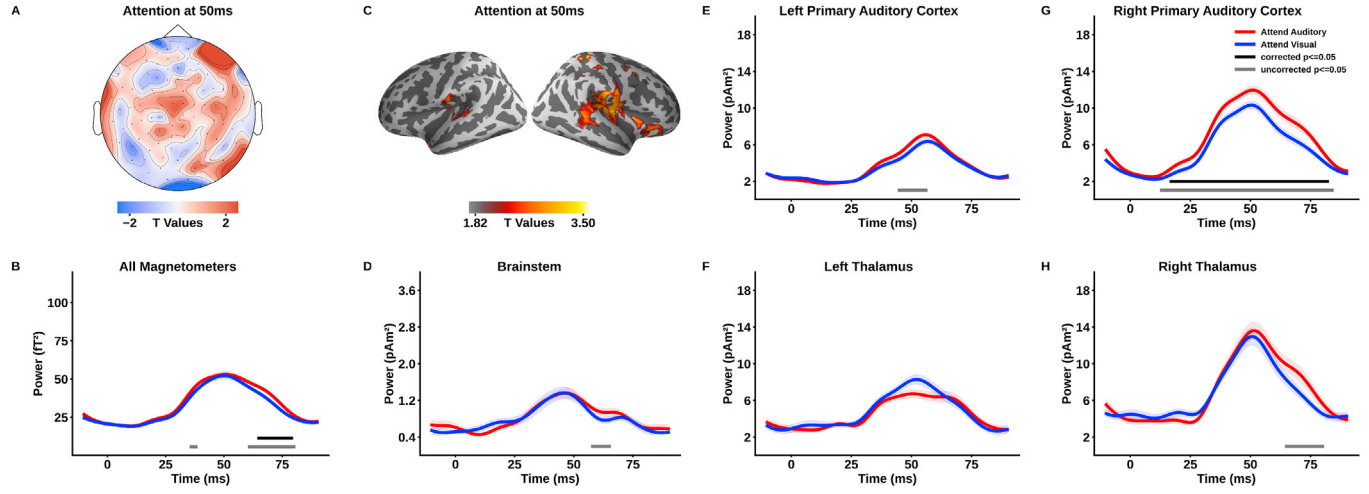

Fig. 3. The attention effect in sensor and source space. A) Topography of the attention effect at the time of maximum power of the FFR. B) Timecourses of the FFR when attention was directed to the auditory domain and the visual domain. Shaded error bars denote the standard error of the mean for within-subjects designs (Morey and Others, 2008). The black bar at the bottom of the panel represents the timeframe in which the FFR was significantly higher when the auditory domain was attended. The gray bar at the bottom represents the samples for which the uncorrected p-value of the *t*-test was below 0.05. C) Source reconstruction of the attention effect. D-H) Timecourse of the FFRs to both conditions. For details, refer to the description of panel B.

was exclusive to the right primary auditory cortex ($p = 0.004$). As suggested descriptively by Fig. 3 data for the right thalamus show a trend towards significance ($p = 0.079$). The left thalamus ($p = 0.754$), the brainstem ($p = 0.238$) and the left primary auditory cortex ($p = 0.138$) did not show any significant attention effect.

These results strongly indicate that attentional processes are represented in cortical components of the FFR while subcortical components remain unaffected.

4. Discussion

It is commonly accepted that the FFR can be used as a proxy to subcortical activity which is otherwise hard to detect in the MEG and EEG (Chandrasekaran and Kraus, 2010; Skoe and Kraus, 2010). The rationale behind this assumption is that only subcortical areas exhibit the strict phase-locking behavior at frequencies above 100 Hz (corresponding to the typical F0) that are commonly used for the stimuli and that the stimulus to response latency is too early for cortical generators (Skoe and Kraus, 2010; Wallace et al., 2000). These assumptions have been recently challenged by a study by Coffey et al. (2016b) that shows strong cortical contributions to the FFR and by studies showing that the auditory cortex reacts to sound stimulation as early as 8–9 ms after stimulus onset (Brugge et al., 2009, 2008; Liegeois-Chauvel et al., 1991). The quasi-automatic attribution of experimental effects on properties of the FFR to subcortical areas thus needs to be revisited.

The FFR has been widely used to study top-down effects of attention on subcortical auditory areas with inconsistent results (Forte et al., 2017; Galbraith et al., 2003; Hoormann et al., 2004; Lehmann and Schönwiesner, 2014; Varghese et al., 2015). Yet, none of these studies used current source projection algorithms to estimate the location of the generators of the reported signals and only some (Forte et al., 2017; Hoormann et al., 2004; Russo et al., 2004) showed the temporal dynamics. The current study is the first that uses the unique strength of the MEG — the combination of its excellent temporal resolution and good spatial resolution — to scrutinize the spatial location of a possible attention-related effect on the FFR without assuming the location of its generators a priori. In sensor space, the attention effect is found considerably later than the FFR, already pointing towards cortical generators. In fact, the simple FFR activation as well as the attention effects outlast the actual period of stimulation, arguing for some reverberatory processes. Overall, the source space analysis confirms the sensor-level finding but also significantly expands it. Firstly, we show next to subcortical generators of the FFR also strong contributions of auditory cortex. This part of the study confirms that the FFR can be detected using MEG (Coffey et al., 2016b) as well as recent findings that the origin of the FFR is not restricted to subcortical areas (Coffey et al., 2016b; Wallace et al., 2000). Also the temporal evolution of the FFR in line with the study by Coffey and colleagues, with a peak reached at ~50 ms. These results may point to indeed an earlier "feedforward" projection of phase-locked activity involving the brainstem, whereas the later portions of the FFR (including those following the stimulus offset) may be more driven by cortico-thalamic interactions. These aspects are beyond the scope of the current study, but open up interesting perspectives in future research on the FFR. Most importantly, however, apart from largely confirming the FFR generating structures as suggested by Coffey and colleagues, we show that only the right primary auditory cortex shows a significant effect of attention.

The source space analysis of the FFR shows a quite widespread pattern of activation, including non-auditory regions in parietal and prefrontal cortex. The depth-weighted MNE is notorious for showing a rather dispersed activation pattern even for originally focal sources (Lin et al., 2006). It is thus debatable whether these activations are real or spurious. However, the estimate of the location of the peak activity is sufficiently accurate (<1 cm) and lies within the inherent limitations of the MEG (Lin et al., 2006). In the case of the present study, the location of the maxima of the sources further coincide well with the results by Coffey et al. (2016b).

Of course, our results do not disprove the presence of attention-related effects on subcortical regions in general and on subcortical generators of the FFR in particular. Sufficient evidence for attention effects in auditory subcortical areas and even the cochlea is available (Giard et al., 1994; Maison et al., 2001; Raizada and Poldrack, 2007; Riecke et al., 2018; Rinne et al., 2008; Slee and David, 2015; Wittekindt et al., 2014). The perfectly regular stimulus presentation at 11.1 Hz might have led to cortical entrainment, boosting the signal-to-noise ratio of the cortical generators. The fundamental frequency of the stimulus was at the border of what is commonly considered to be slow enough to be followed by the cortex (Chandrasekaran and Kraus, 2010; Holmes et al., 2018; Kuwada et al., 2002), leading to the possibility that cortical signals might have masked subcortical ones (see, e.g. Varghese et al., 2015). Another possible explanation, also put forward by (Varghese et al., 2015) is that only specific areas of the brainstem are actually affected by the attentional modulation. The FFR on the other hand is generated by complex interactions between various brainstem and cortical regions (Coffey et al., 2016b; Skoe and Kraus, 2010). Modulations of only a small and specific subset of these regions might not be enough to affect the generated signal, especially when measured with the MEG and/or EEG.

Existing reports on the presence or absence of attentional effects on the FFR used EEG setups that strongly assumed the absence of cortical generators to the FFR (Galbraith et al., 2003; Gutschalk et al., 2008; Hoormann et al., 2004; Lehmann and Schönwiesner, 2014; Varghese et al., 2015). The most prominent "optimization" of the recording setup was that only very few electrodes were used. Yet, recent results strongly suggest that using multi-electrode settings are beneficial: Different EEG montages lead to slightly different outcomes (Coffey et al., 2016a). In addition, separate independent and behaviorally relevant sources can be extracted from the FFR (Zhang and Gong, 2019). Strong cortical contributions, as shown by our results, add further spatial variance. It is thus very likely that the small number of electrodes and their possibly inconsistent locations would be highly relevant and could, at least in part, explain the inconsistent results.

To conclude, by recording the FFR with the MEG at high temporal and good spatial resolution during a cross-modal attention task and using state-of-the-art source projection techniques, we confirm that the cortical generators of the FFR exist and demonstrate for the first time that they are modulated by attention. The lack of an a-priori assumption on the generators of the FFR allowed us to provide a more differentiated perspective on the underlying sources of the FFR and its role in auditory processing. Our results strongly suggest that high-density recording and source projection techniques should be used in future research to disentangle the diverse contributions from cortical and subcortical regions.

Acknowledgements

The authors wish to thank David Opferkuch and Manfred Seifter for their assistance during the collection of the data. We would like to also thank Hayley Prins for proofreading the manuscript.

Appendix A. Supplementary data

Supplementary data to this article can be found online at https://doi.org/10.1016/j.neuroimage.2019.116185.

References

Akalin-Acar, Z., Gençer, N.G., 2004. An advanced boundary element method (BEM) implementation for the forward problem of electromagnetic source imaging. Phys. Med. Biol. 49, 5011–5028.

Akhoun, I., Gallégo, S., Moulin, A., Ménard, M., Veuillet, E., Berger-Vachon, C., Collet, L., Thai-Van, H., 2008. The temporal relationship between speech auditory brainstem responses and the acoustic pattern of the phoneme/ba/in normal-hearing adults. Clin. Neurophysiol. 119, 922–933.

Batra, R., Kuwada, S., Maher, V.L., 1986. The frequency-following response to continuous tones in humans. Hear. Res. 21, 167–177.
Bedna, J., n.d. Colorcet. Github.
Bigdely-Shamlo, N., Mullen, T., Kothe, C., Su, K.-M., Robbins, K.A., 2015. The PREP pipeline: standardized preprocessing for large-scale EEG analysis. Front. Neuroinf. 9, 16.
Boston, J.R., Møller, A.R., 1985. Brainstem auditory-evoked potentials. Crit. Rev. Biomed. Eng. 13, 97–123.
Brainard, D.H., 1997. The Psychophysics toolbox. Spat. Vis. 10, 433–436.
Brodbeck, C., n.d. Eelbrain. Github.
Brugge, J.F., Nourski, K.V., Oya, H., Reale, R.A., Kawasaki, H., Steinschneider, M., Howard 3rd, M.A., 2009. Coding of repetitive transients by auditory cortex on Heschl's gyrus. J. Neurophysiol. 102, 2358–2374.
Brugge, J.F., Volkov, I.O., Oya, H., Kawasaki, H., Reale, R.A., Fenoy, A., Steinschneider, M., Howard 3rd, M.A., 2008. Functional localization of auditory cortical fields of human: click-train stimulation. Hear. Res. 238, 12–24.
Chandrasekaran, B., Kraus, N., 2010. The scalp-recorded brainstem response to speech: neural origins and plasticity. Psychophysiology 47, 236–246.
Chandrasekaran, B., Skoe, E., Kraus, N., 2014. An integrative model of subcortical auditory plasticity. Brain Topogr. 27, 539–552.
Choi, I., Rajaram, S., Varghese, L.A., Shinn-Cunningham, B.G., 2013. Quantifying attentional modulation of auditory-evoked cortical responses from single-trial electroencephalography. Front. Hum. Neurosci. 7, 115.
Coffey, E.B.J., Colagrosso, E.M.G., Lehmann, A., Schönwiesner, M., Zatorre, R.J., 2016. Individual differences in the frequency-following response: relation to pitch perception. PLoS One 11, e0152374.
Coffey, E.B.J., Herholz, S.C., Chepesiuk, A.M.P., Baillet, S., Zatorre, R.J., 2016. Cortical contributions to the auditory frequency-following response revealed by MEG. Nat. Commun. 7, 11070.
Don, M., Eggermont, J.J., 1978. Analysis of the click-evoked brainstem potentials in man unsing high-pass noise masking. J. Acoust. Soc. Am. 63, 1084–1092.
Dragicevic, C.D., Aedo, C., León, A., Bowen, M., Jara, N., Terreros, G., Robles, L., Delano, P.H., 2015. The olivocochlear reflex strength and cochlear sensitivity are independently modulated by auditory cortex microstimulation. J. Assoc. Res. Otolaryngol. 16, 223–240.
Eggermont, J.J., Don, M., 1986. Mechanisms of central conduction time prolongation in brain-stem auditory evoked potentials. Arch. Neurol. 43, 116–120.
Eggermont, J.J., Don, M., Brackmann, D.E., 1980. Electrocochleography and auditory brainstem electric responses in patients with pontine angle tumors. Ann. Otol. Rhinol. Laryngol. Suppl. 89, 1–19.
Eggermont, J.J., Salamy, A., 1988. Maturational time course for the ABR in preterm and full term infants. Hear. Res. 33, 35–47.
Felix 2nd, R.A., Gourévitch, B., Portfors, C.V., 2018. Subcortical pathways: towards a better understanding of auditory disorders. Hear. Res. 362, 48–60.
Filipek, P.A., Richelme, C., Kennedy, D.N., Caviness Jr., V.S., 1994. The young adult human brain: an MRI-based morphometric analysis. Cerebr. Cortex 4, 344–360.
Fischl, B., 2012. FreeSurfer. Neuroimage 62, 774–781.
Fischler, M.A., Bolles, R.C., 1981. Random sample consensus: a paradigm for model fitting with applications to image analysis and automated cartography. Commun. ACM 24, 381–395.
Forte, A.E., Etard, O., Reichenbach, T., 2017. The human auditory brainstem response to running speech reveals a subcortical mechanism for selective attention. eLife Sciences 6, e27203.
Frey, J.N., Mainy, N., Lachaux, J.-P., Müller, N., Bertrand, O., Weisz, N., 2014. Selective modulation of auditory cortical alpha activity in an audiovisual spatial attention task. J. Neurosci. 34, 6634–6639.
Fritz, J.B., Elhilali, M., David, S.V., Shamma, S.A., 2007. Auditory attention–focusing the searchlight on sound. Curr. Opin. Neurobiol. 17, 437–455.
Galbraith, G.C., Arbagey, P.W., Branski, R., Comerci, N., Rector, P.M., 1995. Intelligible speech encoded in the human brain stem frequency-following response. Neuroreport 6, 2363–2367.
Galbraith, G.C., Olfman, D.M., Huffman, T.M., 2003. Selective attention affects human brain stem frequency-following response. Neuroreport 14, 735–738.
Giard, M.H., Collet, L., Bouchet, P., Pernier, J., 1994. Auditory selective attention in the human cochlea. Brain Res. 633, 353–356.
Glasser, M.F., Coalson, T.S., Robinson, E.C., Hacker, C.D., Harwell, J., Yacoub, E., Ugurbil, K., Andersson, J., Beckmann, C.F., Jenkinson, M., Smith, S.M., Van Essen, D.C., 2016. A multi-modal parcellation of human cerebral cortex. Nature 536, 171–178.
Gramfort, A., Luessi, M., Larson, E., Engemann, D.A., Strohmeier, D., Brodbeck, C., Goj, R., Jas, M., Brooks, T., Parkkonen, L., Hämäläinen, M., 2013. MEG and EEG data analysis with MNE-Python. Front. Neurosci. 7, 267.
Gramfort, A., Luessi, M., Larson, E., Engemann, D.A., Strohmeier, D., Brodbeck, C., Parkkonen, L., Hämäläinen, M.S., 2014. MNE software for processing MEG and EEG data. Neuroimage 86, 446–460.
Greenberg, S., 1980. WPP, No. 52: Temporal Neural Coding of Pitch and Vowel Quality. Working Papers in Phonetics.
Gross, J., Kujala, J., Hamalainen, M., Timmermann, L., Schnitzler, A., Salmelin, R., 2001. Dynamic imaging of coherent sources: studying neural interactions in the human brain. Proc. Natl. Acad. Sci. U.S.A. 98, 694–699.
Gutschalk, A., Micheyl, C., Oxenham, A.J., 2008. Neural correlates of auditory perceptual awareness under informational masking. PLoS Biol. 6, e138.
Hackley, S.A., Woldorff, M., Hillyard, S.A., 1990. Cross-modal selective attention effects on retinal, myogenic, brainstem, and cerebral evoked potentials. Psychophysiology 27, 195–208.
Haegens, S., Nácher, V., Luna, R., Romo, R., Jensen, O., 2011. α-Oscillations in the monkey sensorimotor network influence discrimination performance by rhythmical inhibition of neuronal spiking. Proc. Natl. Acad. Sci. U.S.A. 108, 19377–19382.
Hämäläinen, M.S., Ilmoniemi, R.J., 1994. Interpreting magnetic fields of the brain: minimum norm estimates. Med. Biol. Eng. Comput. 32, 35–42.
Händel, B.F., Haarmeier, T., Jensen, O., 2011. Alpha oscillations correlate with the successful inhibition of unattended stimuli. J. Cogn. Neurosci. 23, 2494–2502.
Holmes, E., Purcell, D.W., Carlyon, R.P., Gockel, H.E., Johnsrude, I.S., 2018. Attentional modulation of envelope-following responses at lower (93-109 Hz) but not higher (217-233 Hz) modulation rates. J. Assoc. Res. Otolaryngol. 19, 83–97.
Hoormann, J., Falkenstein, M., Hohnsbein, J., 2004. Effects of spatial attention on the brain stem frequency-following potential. Neuroreport 15, 1539–1542.
Jas, M., Engemann, D.A., Bekhti, Y., Raimondo, F., Gramfort, A., 2017. Autoreject: automated artifact rejection for MEG and EEG data. Neuroimage 159, 417–429.
Jas, M., Engemann, D., Raimondo, F., Bekhti, Y., Gramfort, A., 2016. Automated rejection and repair of bad trials in MEG/EEG. In: 2016 International Workshop on Pattern Recognition in Neuroimaging (PRNI), pp. 1–4.
Jensen, O., Mazaheri, A., 2010. Shaping functional architecture by oscillatory alpha activity: gating by inhibition. Front. Hum. Neurosci. 4, 186.
Jewett, D.L., Romano, M.N., Williston, J.S., 1970. Human auditory evoked potentials: possible brain stem components detected on the scalp. Science 167, 1517–1518.
King, C., Warrier, C.M., Hayes, E., Kraus, N., 2002. Deficits in auditory brainstem pathway encoding of speech sounds in children with learning problems. Neurosci. Lett. 319, 111–115.
Kleiner, M., Brainard, D., Pelli, D., Ingling, A., Murray, R., Broussard, C., 2007. What's new in psychtoolbox-3. Perception 36, 1–16.
Kovesi, P., 2015. Good Colour Maps: How to Design Them (arXiv [cs.GR]).
Kraus, N., Nicol, T., 2014. The cognitive auditory system: the role of learning in shaping the biology of the auditory system. In: Popper, A.N., Fay, R.R. (Eds.), Perspectives on Auditory Research. Springer New York, New York, NY, pp. 299–319.
Kuwada, S., Anderson, J.S., Batra, R., Fitzpatrick, D.C., Teissier, N., D'Angelo, W.R., 2002. Sources of the scalp-recorded amplitude-modulation following response. J. Am. Acad. Audiol. 13, 188–204.
Lee, A.K.C., Rajaram, S., Xia, J., Bharadwaj, H., Larson, E., Hämäläinen, M.S., Shinn-Cunningham, B.G., 2012. Auditory selective attention reveals preparatory activity in different cortical regions for selection based on source location and source pitch. Front. Neurosci. 6, 190.
Lehmann, A., Schönwiesner, M., 2014. Selective attention modulates human auditory brainstem responses: relative contributions of frequency and spatial cues. PLoS One 9, e85442.
Liegeois-Chauvel, C., Musolino, A., Chauvel, P., 1991. Localization of the primary auditory area in man. Brain 114 (Pt 1A), 139–151.
Lin, F.-H., Witzel, T., Ahlfors, S.P., Stufflebeam, S.M., Belliveau, J.W., Hämäläinen, M.S., 2006. Assessing and improving the spatial accuracy in MEG source localization by depth-weighted minimum-norm estimates. Neuroimage 31, 160–171.
Liu, L.-F., Palmer, A.R., Wallace, M.N., 2006. Phase-locked responses to pure tones in the inferior colliculus. J. Neurophysiol. 95, 1926–1935.
Maison, S., Micheyl, C., Collet, L., 2001. Influence of focused auditory attention on cochlear activity in humans. Psychophysiology 38, 35–40.
Maris, E., Oostenveld, R., 2007. Nonparametric statistical testing of EEG- and MEG-data. J. Neurosci. Methods 164, 177–190.
Marsh, J.T., Brown, W.S., Smith, J.C., 1974. Differential brainstem pathways for the conduction of auditory frequency-following responses. Electroencephalogr. Clin. Neurophysiol. 36, 415–424.
Mazaheri, A., van Schouwenburg, M.R., Dimitrijevic, A., Denys, D., Cools, R., Jensen, O., 2014. Region-specific modulations in oscillatory alpha activity serve to facilitate processing in the visual and auditory modalities. Neuroimage 87, 356–362.
Møller, A.R., Burgess, J., 1986. Neural generators of the brain-stem auditory evoked potentials (BAEPs) in the rhesus monkey. Electroencephalogr. Clin. Neurophysiol. 65, 361–372.
Møller, A.R., Jannetta, P.J., 1983. Interpretation of brainstem auditory evoked potentials: results from intracranial recordings in humans. Scand. Audiol. 12, 125–133.
Møller, A.R., Jannetta, P.J., Møller, M.B., 1981. Neural generators of brainstem evoked potentials. Results from human intracranial recordings. Ann. Otol. Rhinol. Laryngol. 90, 591–596.
Møller, M.B., Møller, A.R., 1983. Brainstem auditory evoked potentials in patients with cerebellopontine angle tumors. Ann. Otol. Rhinol. Laryngol. 92, 645–650.
Morey, R.D., Others, 2008. Confidence intervals from normalized data: a correction to Cousineau (2005). Reason 4, 61–64.
Musacchia, G., Sams, M., Skoe, E., Kraus, N., 2007. Musicians have enhanced subcortical auditory and audiovisual processing of speech and music. Proc. Natl. Acad. Sci. U.S.A. 104, 15894–15898.
Parkkonen, L., Fujiki, N., Mäkelä, J.P., 2009. Sources of auditory brainstem responses revisited: contribution by magnetoencephalography. Hum. Brain Mapp. 30, 1772–1782.
Raizada, R.D.S., Poldrack, R.A., 2007. Challenge-driven attention: interacting frontal and brainstem systems. Front. Hum. Neurosci. 1, 3.
Riecke, L., Peters, J.C., Valente, G., Poser, B.A., Kemper, V.G., Formisano, E., Sorger, B., 2018. Frequency-specific attentional modulation in human primary auditory cortex and midbrain. Neuroimage 174, 274–287.
Rinne, T., Balk, M.H., Koistinen, S., Autti, T., Alho, K., Sams, M., 2008. Auditory selective attention modulates activation of human inferior colliculus. J. Neurophysiol. 100, 3323–3327.
Rouiller, E., de Ribaupierre, Y., de Ribaupierre, F., 1979. Phase-locked responses to low frequency tones in the medial geniculate body. Hear. Res. 1, 213–226.

Russo, N., Nicol, T., Musacchia, G., Kraus, N., 2004. Brainstem responses to speech syllables. Clin. Neurophysiol. 115, 2021–2030.
Salo, E., Salmela, V., Salmi, J., Numminen, J., Alho, K., 2017. Brain activity associated with selective attention, divided attention and distraction. Brain Res. 1664, 25–36.
Seidman, L.J., Faraone, S.V., Goldstein, J.M., Goodman, J.M., Kremen, W.S., Toomey, R., Tourville, J., Kennedy, D., Makris, N., Caviness, V.S., Tsuang, M.T., 1999. Thalamic and amygdala-hippocampal volume reductions in first-degree relatives of patients with schizophrenia: an MRI-based morphometric analysis. Biol. Psychiatry 46, 941–954.
Skoe, E., Kraus, N., 2010. Auditory brain stem response to complex sounds: a tutorial. Ear Hear. 31, 302–324.
Slee, S.J., David, S.V., 2015. Rapid task-related plasticity of spectrotemporal receptive fields in the auditory midbrain. J. Neurosci. 35, 13090–13102.
Smith, S.M., Nichols, T.E., 2009. Threshold-free cluster enhancement: addressing problems of smoothing, threshold dependence and localisation in cluster inference. Neuroimage 44, 83–98.
Stipdonk, L.W., Weisglas-Kuperus, N., Franken, M.-C.J., Nasserinejad, K., Dudink, J., Goedegebure, A., 2016. Auditory brainstem maturation in normal-hearing infants born preterm: a meta-analysis. Dev. Med. Child Neurol. 58, 1009–1015.
Suga, N., 2008. Role of corticofugal feedback in hearing. J. Comp. Physiol. A Neuroethol. Sens. Neural Behav. Physiol. 194, 169–183.
Terreros, G., Delano, P.H., 2015. Corticofugal modulation of peripheral auditory responses. Front. Syst. Neurosci. 9, 134.
Tichko, P., Skoe, E., 2017. Frequency-dependent fine structure in the frequency-following response: the byproduct of multiple generators. Hear. Res. 348, 1–15.
Tzounopoulos, T., Kraus, N., 2009. Learning to encode timing: mechanisms of plasticity in the auditory brainstem. Neuron 62, 463–469.
Uusitalo, M.A., Ilmoniemi, R.J., 1997. Signal-space projection method for separating MEG or EEG into components. Med. Biol. Eng. Comput. 35, 135–140.
van Straaten, H.L., 1999. Automated auditory brainstem response in neonatal hearing screening. Acta Paediatr. Suppl. 88, 76–79.
Van Veen, B.D., van Drongelen, W., Yuchtman, M., Suzuki, A., 1997. Localization of brain electrical activity via linearly constrained minimum variance spatial filtering. IEEE Trans. Biomed. Eng. 44, 867–880.
Varghese, L., Bharadwaj, H.M., Shinn-Cunningham, B.G., 2015. Evidence against attentional state modulating scalp-recorded auditory brainstem steady-state responses. Brain Res. 1626, 146–164.
Wallace, M.N., Anderson, L.A., Palmer, A.R., 2007. Phase-locked responses to pure tones in the auditory thalamus. J. Neurophysiol. 98, 1941–1952.
Wallace, M.N., Rutkowski, R.G., Shackleton, T.M., Palmer, A.R., 2000. Phase-locked responses to pure tones in Guinea pig auditory cortex. Neuroreport 11, 3989–3993.
Weise, A., Hartmann, T., Schröger, E., Weisz, N., Ruhnau, P., 2016. Cross-modal distractors modulate oscillatory alpha power: the neural basis of impaired task performance. Psychophysiology. https://doi.org/10.1111/psyp.12733.
Winer, J.A., 2006. Decoding the auditory corticofugal systems. Hear. Res. 212, 1–8.
Wittekindt, A., Kaiser, J., Abel, C., 2014. Attentional modulation of the inner ear: a combined otoacoustic emission and EEG study. J. Neurosci. 34, 9995–10002.
Woldorff, M., Hansen, J.C., Hillyard, S.A., 1987. Evidence for effects of selective attention in the mid-latency range of the human auditory event-related potential. Electroencephalogr. Clin. Neurophysiol. Suppl. 40, 146–154.
Worden, F.G., Marsh, J.T., 1968. Frequency-following (microphonic-like) neural responses evoked by sound. Electroencephalogr. Clin. Neurophysiol. 25, 42–52.
Zhang, X., Gong, Q., 2019. Frequency-following responses to complex tones at different frequencies reflect different source configurations. Front. Neurosci. 13, 130.